Gellan Fluid Gel as a Versatile Support Bath Material for Fluid Extrusion Bioprinting

*Ashley M. Compaan, Kaidong Song, Yong Huang**

Ashley M. Compaan[1], Kaidong Song[2], Yong Huang[1, 2, 3,*]

[1]Department of Materials Science and Engineering, University of Florida, Gainesville, FL 32611, USA.

[2]Department of Mechanical and Aerospace Engineering, University of Florida, Gainesville, FL 32611, USA.

[3]Department of Biomedical Engineering, University of Florida, Gainesville, FL 32611, USA.

*Corresponding author, Department of Mechanical and Aerospace Engineering, University of Florida, Gainesville, FL 32611, USA, Phone: 001-352-392-5520, Fax: 001- 352-392-7303, Email: yongh@ufl.edu.

Keywords: hydrogel, biomedical applications, bioprinting, gellan, freeform

Abstract

Biomedical applications of three-dimensional (3D) printing demand complex hydrogel-based constructs laden with living cells. Advanced support materials facilitate the fabrication of such constructs. This work demonstrates the versatility and utility of gellan fluid gel as a support bath material for fabricating freeform 3D hydrogel constructs from a variety of

materials. Notably, the gellan fluid gel support bath can supply sensitive biological cross-linking agents such as enzymes to printed fluid hydrogel precursors for mild covalent hydrogel cross-linking. This mild fabrication approach is suitable for fabricating cell-laden gelatin-based constructs in which mammalian cells can form intercellular contacts within hours of fabrication; cellular activity is observed over several days within printed constructs. In addition, gellan is compatible with a wide range of ionic and thermal conditions, which makes it a suitable support material for ionically cross-linked structures generated by printing alginate-based ink formulations as well as thermosensitive hydrogel constructs formed from gelatin. Ultra-violet irradiation of printed structures within the support bath is also demonstrated for photoinitiated cross-linking of acrylated ink materials. Furthermore, gellan support material performance in terms of printed filament stability and residual support material on constructs is found to be comparable and superior, respectively, to previously reported support materials.

1. Introduction

Tissue engineering is a field which seeks to recapitulate structural and functional features of living tissues in engineered constructs. There are a variety of purposes for these constructs: mimicking healthy and disease states to better understand diseases, modeling physiological responses for drug discovery and validation, and promoting regeneration of damaged tissue in vivo. Additive manufacturing, or three-dimensional (3D) printing,[1] has proven to be a particularly useful tool for fabricating engineered tissue constructs.[2-6] Its unique capacity for rapid, customized fabrication with the potential for material heterogeneity and ability to incorporate living cells is important for construct design optimization and patient-specific treatments as this technology is translated to the clinic.

Extrusion bioprinting is the most widely adopted 3D printing technology for biomedical applications because it is efficient (in both time and materials), easy to control, and compatible with a wide range of build materials. Recently, various types of extrusion 3D printing which rely on high performance support bath materials have been reported.[7-15] In general, these support materials are yield stress materials, which means that they behave as elastic solids at rest but can be liquefied by applying sufficient stress; once liquefied, they are often shear thinning. Importantly, these support materials revert to solid-like behavior when the applied stress drops below the yield stress. This behavior has been exploited to facilitate truly freeform 3D printing: the support material provides a 3D environment in which filaments or droplets of a build material can be deposited in gravity-defying spatial arrangements. The motion of the nozzle and force exerted by material deposition locally liquefy the support material, and as soon as the material is deposited, it is trapped in place as the surrounding support material reverts to solid-like behavior. Thus, even though the deposited material may be fluid, it retains the deposited shape since it is constrained by the surrounding support material.

Although previously reported support materials are suitable for some applications, they have limitations and more versatile yield stress support materials are needed, particularly for biofabrication of soft biopolymer constructs. Yield stress behavior arises in a wide variety of complex fluid systems ranging from block copolymer blends [15] to inorganic colloids [12,13] to jammed microgels.[7, 8, 10, 11, 14] Each has limitations for biofabrication applications, however. Block copolymers [15] such as commercially available Kraton products have limited biocompatibility and may be difficult to separate from printed structures. While inorganic colloids such as Laponite [12, 13] are highly biocompatible, removing residual support material may be a challenge and they may sequester or inactivate macromolecules utilized in the printing process, as shown in this work. Carbopol [7, 10, 11] is a synthetic transparent jammed

microgel system which is unfortunately incompatible with multivalent cations and sensitive to ionic strength in general. Gelatin microgel support materials [8] are sensitive to temperature while agar microgels are unsuitable for detailed structures.[14] Thus, a more versatile and robust support material which is easy to separate from printed constructs and compatible with a wide range of printed materials, cross-linking mechanisms, and printing conditions is needed.

This work explores the potential of gellan fluid gel materials as support materials for bath-enabled extrusion 3D printing. Gellan is an extracellular microbial polysaccharide which has been commercialized as a gelling agent since it forms robust tunable hydrogels under mild conditions. Gel properties can be adjusted by a range of factors: gellan concentration, dissolved additives such as salts or sugars, and processing conditions. Gellan hydrogels can also be processed to form so-called fluid gels, which are jammed dispersions of hydrogel microparticles.

The gellan fluid-gel enabled printing process is illustrated in **Figure** 1. The structure is fabricated by extruding build material (referred to as ink herein) within a gellan microgel support bath, as shown in **Figure** 1 and **Movie** M1. First, a reservoir is filled with the jammed gellan fluid gel support material, which behaves as a solid when at rest as shown in **Figure** 1(a). To create features in the support material, an extrusion tip is inserted into the support material so that it can deposit ink filaments as it travels along designed paths in the x, y, and z directions in the printing reservoir. As the tip travels, the bulk support material liquefies because the microgels deform and slide past one another, as shown in **Figure** 1(b). This liquefied region allows the ink to flow out of the extrusion tip. As the tip moves away, the microgels revert to a jammed solid-like configuration and the printed material is trapped as illustrated in **Figure** 1(c). This solid-fluid-solid transition is confined to a small region around the traveling nozzle since the microgels deform and rearrange to absorb energy rather than transferring it over long distances. This process continues until the entire structure is printed,

as shown in **Figure** 1(d). Then, the deposited ink structure is cured or cross-linked to form an intact structure and the support material is washed away to obtain a construct suitable for maturation and/or characterization as shown in **Movie** M2.

2. Results and Discussion

2.1 Gellan as a support material for extrusion bioprinting

Gellan, as shown in **Figure** 2(a), is a linear anionic microbial polysaccharide which is gaining popularity in a variety of fields including tissue engineering, drug delivery, and food science.[16-18] The repeat unit is a tetrasaccharide sequence which includes two β-D-glucose residues, one β-D-glucuronate residue, and one α-L-rhamnose residue. The native gellan biopolymer contains acyl groups which are removed to produce the widely-used low acyl version of the biopolymer, which is the material investigated in this work. At high temperature, gellan molecules exist as random coils in aqueous solution; upon cooling, some regions of the polymer adopt a helical conformation and aggregate to form junction zones, resulting in a bulk hydrogel by physical gel formation, as shown schematically in **Figure** 2(b). Low acyl gellan forms clear, brittle hydrogels which can be easily processed into fluid gels.[19] Fluid gels are microgel dispersions formed by shearing or fragmenting hydrogels during or after gelation. They have a yield stress since they are jammed microgel systems; the yield stress is due to the threshold energy required to make the microgels deform and slide past one another so that the bulk material can flow. Although low-acyl gellan can form stiff gels without added salt, the gel properties can be modulated by changing the concentration and composition of added ions as well as the pH. For this work, gellan fluid gel is prepared in a physiological buffer, phosphate buffered saline (PBS), to prevent osmotic shock to printed cells, stabilize the pH, and match the ionic strength of the ink formulations to minimize swelling. Bulk gels are fragmented by passing through stainless steel mesh, resulting in a smoothly flowing yield stress fluid. Microscopic examination of the dispersion shows

irregular microgel particles with typical dimensions of 20-40 μm, as shown in **Figure** 2(c) and (d), which is consistent with other reports of gellan fluid gel microstructure.[20] In all cases, the particle sizes and morphologies are similar; this is attributed to the similar gel fragmentation process which determines the particle size.

Rheological characterization of the support material was carried out to quantify the yield stress behavior of the prepared support materials: 0.5% w/v gellan at ambient temperature, 0.5% w/v gellan + 0.1% w/v $CaCl_2$•$2H_2O$ at ambient temperature and at 37°C, and 1.0% w/v gellan at ambient temperature. Steady shear strain rate sweep data was fit to the Herschel-Bulkley model of yield stress fluid behavior, $\sigma = \sigma_0 + K\dot{\gamma}^n$, where σ is the total stress, σ_0 is the yield stress, $\dot{\gamma}$ is the shear rate, and K and n are fitting parameters. Notably, n is the flow index and indicates the intensity of shear thinning behavior; $n=1$ for materials where the apparent viscosity is independent of shear rate, while $n<1$ for shear thinning materials and $n>1$ for shear thickening materials. **Figure** 2(d-f) show the steady and oscillatory shear rheometry data in graphic form; fitting parameters are listed in **Table** 1, and **Figure** S1(a) shows the low shear plateau behavior for the same set of materials. **Figure** 2(e) highlights the strong shear thinning behavior under steady shear, while **Figure** 2(f) shows the transition from solid-like (G'>G") to fluid like (G'<G") behavior in oscillatory strain sweep measurements. **Figure** 2(g) shows that the transition is reversible with essentially similar solid-like and fluid-like behavior under low and high shear strains as the sample subjected to cycles of low and high strain oscillatory shear. The printing support material (0.5% gellan fluid gel prepared in PBS and supplemented with 0.1% $CaCl_2$•$2H_2O$) was compared to 0.5% gellan and 1.0% gellan, both in PBS without added calcium. Calcium was included to modify the support material rheology by slightly altering the microgel properties;[18,20] in some cases it also served to limit diffusion for some ink materials such as formulations including alginate by slow partial cross-linking. Figure S1(b) shows that the behavior of all support formulations

under small amplitude oscillatory shear is similar and more solid-like than fluid-like (G'>G") over the range of tested frequencies, which is typical of yield stress materials. [7, 10-13, 15]

As seen from **Table** 1, the yield stresses are 1.4 Pa for 0.5% gellan without added calcium, 1.1 Pa and 1.9 Pa for 0.5% gellan with added calcium at ambient temperature and 37°C respectively, and 1.5 Pa for 1.0% gellan. The properties of these formulations fall within the range of properties for other reported yield stress support materials.[7, 12, 13, 15] A higher gellan concentration leads to stiffer gels and correspondingly higher yield stress.[21] These observed stress variations are consistent with literature regarding gellan fluid gels and microgel dispersions: while the addition of calcium might be expected to stiffen the gel particles and therefore raise the yield stress,[22] they are already effectively stabilized by ions from PBS and the addition of calcium actually reduces the yield stress; this may be attributed to shrinkage of the gel particles and/or reduction of entangled dangling chains as a result of strong interactions with calcium ions. On the other hand, 37°C is close to observed critical temperatures for aggregation of helical gellan with added calcium,[23, 24] so warming the gellan gel to this temperature slightly destabilizes the helical conformation and makes the particles softer and more able to interact with one another, resulting in a higher yield stress since the overall material can absorb more energy without initiating flow. A slight increase in G' is also observed for 0.5% gellan with added calcium at 37°C as shown in Figure S1(b). Gellan particles may also swell at elevated temperature, reducing the amount of lubricating free water in the bulk material and therefore raising the yield stress. It is noteworthy that the addition of calcium strongly influences the flow index of gellan microgel dispersions, reducing it from ~0.5 to ~0.3. In other words, the addition of calcium makes the gellan fluid gel much more shear thinning and therefore easier to separate from printed constructs since the gel material fluidizes more readily in response to agitation or flow. By comparison, the flow index is typically 0.4-0.6 for Carbopol preparations under physiological conditions [25-27]

and 0.3-0.9 for Laponite RD in tap water.[27] The reduced flow index upon addition of calcium may be related to calcium-mediated tight packing of helical regions, making the individual microgels slightly more compact and reducing the concentration of free or dangling gellan chains between microgel particles which would hinder bulk flow. Thus, there would be less friction between microgels and a stronger shear thinning behavior since the irregular gel particles could rotate freely under applied shear to minimize their resistance to flow.

2.2 Printing procedure

The bath-supported microextrusion process is illustrated in **Figure** 1. As described earlier, material is deposited along designed paths as the tip travels to create a supported structure layer by layer. After the entire structure is printed, gel formation takes place within the support bath to stabilize the structure before further processing.

Regarding ink materials, this work focuses on hydrogel materials which are formed by cross-linking fluid precursors after printing (printing-then-gelation); ink and support bath materials are summarized in **Table** S1 (Supporting Information). after printing (printing-then-gelation); ink and support bath materials are summarized in **Table** S1 (Supporting Information). The printing-then-gelation terminology emphasizes the formation of freestanding liquid objects first with gelation after printing is complete. It encompasses both freeform reversible embedding of suspended hydrogels (FRESH)[8] and writing in a microgel medium.[7] These previous process designations [7, 8] for the printing process focus on different aspects of support bath materials involved instead of the common printing procedure itself: FRESH emphasizes the ability to liquefy the gelatin-based support material, while writing in the granular gel medium emphasizes the creation of 3D features within a specific microgel-based support material. In essence, these two processes and the proposed process all belong to the printing-then-gelation category. Thus, printing-then-gelation/solidification is used herein to better represent the nature of the printing procedure itself. Cross-links may be physical,

ionic, and/or covalent – examples herein include the covalent cross-links formed by enzymatic action on specific functional groups by using transglutaminase (TG) to gel native gelatin, the physical gelation of gelatin upon cooling, the ionic gelation of alginate (and other polysaccharides) in the presence of multivalent cations, and photoinitiated covalent cross-linking of poly(ethylene glycol) diacrylate (PEGDA) by free radical polymerization. For conventional 3D printing approaches, the deposited material must immediately solidify in the desired shape. Because the bath-supported printing methodology largely decouples the shape fidelity of the printed construct from the speed of solidification, it can be used in conjunction with slow solidification processes, enabling printing-then-solidification of complex constructs and greatly extending the range of printable materials. This also mitigates mechanical weakness and anisotropy due to interfaces between printed regions since the deposited material remains fluid long enough to fuse into a cohesive structure before cross-linking takes place.[10, 11]

Various types of constructs are fabricated herein to demonstrate the ability to print shells and solid objects as well as demonstrate cell encapsulation. The focus of this work is on the support bath material versatility in terms of build material options, and the main goal is to demonstrate noteworthy and valuable features of this support material in contrast with previously-reported support material options. For example, Carbopol is a synthetic transparent jammed microgel system[7,10] which is unfortunately incompatible with multivalent cations and sensitive to ionic strength in general; in contrast, gellan is an effective support material at physiological ionic strength and its rheological properties only vary slightly in response to multivalent ions. Gelatin microgel support materials[8] are sensitive to temperature while agar microgels[14] are unsuitable for detailed structures; in contrast, gellan rheology is stable over a range of temperatures and it is a suitable support material for printing solid, porous, and/or thin walled features from a range of build materials as demonstrated herein.

2.2.1 Structures stabilized by enzyme-mediated covalent cross-linking

The suitability of gellan as a support material for enzyme-mediated hydrogel printing was investigated using gelatin as the principal ink component and TG as the enzymatic cross-linking agent. Enzymes are attractive tools for tissue engineering since they are biological catalysts which are usually highly active under physiological conditions with high specificity and low toxicity. Transglutaminases are a family of enzymes which form covalent linkages between protein molecules. A robust microbial TG has been commercialized for food use (modification of food proteins) and has also been utilized in tissue engineering to stabilize and stiffen protein-based hydrogels such as gelatin and collagen.[28-30] Because it is non-toxic, biodegradable, cytocompatible, and does not introduce toxic residues or byproducts (except for trace amounts of ammonia which may be processed through normal metabolic pathways active in cells), and because it can be used to form physiologically stable cell-laden gel constructs from gelatin, which is a cheap and readily available protein derived from collagen, microbial TG is utilized in this study.

Gelatin forms physical hydrogels via physical interactions between helical regions of the protein; however, above approximately 35°C, the hydrogel liquefies as helical regions become random coils. Recent work comparing native gelatin cross-linked by a variety of agents found that TG produced optimal transparent, non-toxic, stable, transparent, degradable, biocompatible structures suitable for *in vitro* and *in vivo* biomedical applications.[31] While chemical modification of gelatin may provide superior control of hydrogel formation and properties, it significantly complicates the material preparation process since the native protein must be modified and purified before use. Also, residual reactants from the modification process, the functional groups themselves, initiators or catalysts, and/or the stimuli required to form a hydrogel from the modified gelatin may negatively impact encapsulated or seeded cells. For example, methacrylated gelatin (GelMA) which can be

photocrosslinked is valuable for thin planar constructs where brief ultraviolet (UV) exposure cures the material homogenously, but consistent results require that the entire structure be exposed to a consistent level of UV radiation. Thus, complex GelMA constructs where one feature overshadows another are difficult or impossible to cross-link homogenously. Furthermore, UV exposure may damage cells so the inconsistent irradiation subjects cells in different regions of the construct to varied amounts of damage. For these reasons, native gelatin is used in this work to avoid these complications and make the process feasible in a wide range of facilities where extensive material modification may not be possible or convenient.

Three gelatin-based ink formulations were evaluated for enzyme-mediated structure formation in a gellan microgel support formulation (0.5% gellan + 0.1% $CaCl_2$•$2H_2O$ + 2% TG): 5% gelatin + 2% alginate, 10% gelatin + 2% alginate, and 4% gelatin + 0.5% gellan + 0.1% $CaCl_2$•$2H_2O$. The printability of pure gelatin solutions is poor due to low viscosity and resulting uncontrolled flow around the extrusion tip, so either 2% w/v alginate or 0.5% gellan fluid gel with 0.1% $CaCl_2$•$2H_2O$ was included to control the ink rheology. For gelatin/alginate inks, two gelatin concentrations (5% and 10%) were utilized to evaluate the differences in printing performance and facilitate mechanical characterization; 0.5% gellan-based ink included 4% w/v gelatin. For biofabrication of soft tissues, it is generally desirable to minimize the gelatin concentration in order to provide a permissive environment for cell extension and tissue development.[29, 32-34] However, other biomedical and engineering applications may call for formulations with higher gelatin content to optimize mechanical or transport properties. Therefore, all three ink formulations are of interest for various applications.

For gelatin/alginate inks, the fabrication temperature was an important parameter; more consistent results were obtained when both ink and support bath were maintained at an

elevated temperature (37°C) than when they were printed in ambient conditions. As a support material, the properties of gellan only vary slightly in this temperature range as observed so it was equally suitable for fabrication at ambient and physiological temperatures. Without active temperature control, the cooling temperature-sensitive ink may result in inconsistent printing performance and clogged printing nozzles, especially with 10% gelatin. This is particularly important for large or complex structures which may require long printing times: heating both the ink and support enables consistent performance over the course of several hours, while at ambient conditions printing performance may deteriorate within one hour. The gelatin/gellan ink formulation was less sensitive to temperature and could be printed under ambient conditions for several hours after initial preparation at 37°C. This is attributed to the microstructure imparted by the gellan fluid gel component which retarded bulk gel formation. Structures formed from each of these ink formulations are shown in **Figure** 3. The overall morphology and print quality is similar for all three formulations, although the gelatin/gellan ink is less transparent than the alginate-based formulations.

One important feature of gellan as a support material is the ability to use sensitive biomolecules during the printing process without loss of activity. This feature is illustrated by comparison with another support material which has been utilized for 3D bioprinting, Laponite. For gelatin structure printing using TG as a cross-linking agent, it is necessary for TG to be present and active in the support bath so that it can diffuse into the printed structure and form covalent cross-links to stabilize the structure for later removal from the support bath. Gellan provides an inert support which supplies active TG to the printed ink, while alternative support materials Laponite EP and Laponite XLG [12, 13] effectively reduce the enzyme activity such that intact covalent hydrogel structures are not formed. Three support material formulations (0.5% gellan gum with 2% TG, 4% Laponite XLG with 2% TG, and 4% Laponite EP with 2% TG) were used to demonstrate this difference using the procedure

illustrated in **Figure** 4(a) to produce cast gelatin discs. This approach enables evaluation of enzymatic cross-linking efficiency without variation related to printing in the different support materials. Each support material is prepared and loaded in a vial as shown in Figure 4(a(i)), then gelatin solution is gently added atop the support material as shown in Figure 4(a(i)) and the vial is incubated to permit enzymatic cross-linking (if active enzyme is available from the support material) as shown in Figure 4(a(iii)). Then, the entire vial is chilled as shown in Figure 4(a(iv)); this results in physical cross-linking and allows the cast gelatin disc to be separated from the support material whether it is covalently cross-linked or not. Finally, the gelatin disc is rinsed to remove residual support material and warmed to 37°C as shown in Figure 4(a(v)). This causes physically cross-linked discs to liquefy but does not affect the shape of covalently cross-linked gelatin discs.In all cases, well-defined gelatin discs are obtained after chilling the samples as shown in **Figure** 4(b(i)); this is expected since gelatin forms physical gels at 4°C. Upon warming to 37°C, only the gellan supported gel remains intact (**Figure** 4(b(iii))). The XLG supported gel dissolves almost entirely, except for a thin, fragile disc attributed to the formation of a gelatin-Laponite composite at the interface (not shown). The gelatin disc formed in contact with TG-supplemented Laponite EP turns into a soft shapeless mass upon warming, as shown in **Figure** 4(b(ii)); this is consistent with limited covalent cross-linking sufficient to make a cohesive object but unsuitable for defined structures. These results indicate that Laponite formulations effectively sequester or denature TG, resulting in very low enzyme activity towards printed material. This is likely due to strong interactions between Laponite and TG which entrap TG in the support rather than allowing free diffusion into the printed material. Similar Laponite-based slow-release phenomena have been exploited elsewhere for controlled delivery of pharmaceuticals and growth factors;[35] however, for 3D bioprinting this behavior is undesirable since it prevents TG from acting on the ink rapidly enough to be useful for fabrication of mechanically stable

structures. On the other hand, gellan hydrogels typically show burst release drug delivery behavior;[17, 36, 37] such rapid delivery of TG to the adjacent gelatin precursor fluid accounts for the thermal and mechanical stability of the gelatin discs.

The printing process often produces objects with anisotropic mechanical properties due to interfaces between layers and regions.[38] To evaluate the effect of the printing process on the mechanical properties of enzyme cross-linked gel structures (**Figure** 5(a)), the effective stiffness (**Figure** 5(b)) is quantified for three mechanical test specimen designs: printed conventional dogbone structures[38] and two rectangular structures with print paths parallel to or perpendicular to the force applied during testing. Rectangular specimens are designed to evaluate print path effects using a single layer in the gage regions, while the traditional dogbone structure is three layers thick to minimize printing effects. These specimens were fabricated using the 10% gelatin/ 2% alginate ink formulation to generate structures with relatively high effective stiffness (for ease of handling) and avoid any complications associated with the microstructure imparted by gellan in the gelatin/ gellan ink formulation. The gelatin/alginate ink formulations form continuous, homogeneous gelatin networks with entrapped alginate molecules; gelatin/gellan ink, on the other hand, forms microgel-reinforced composite solids in which embedded microgels significantly affect the mechanical properties and complicate evaluation of printing effects, so it was not evaluated in this section. For cross-linking, the support bath contained 2.0% TG as for other printed constructs using this ink formulation.

Measured effective stiffness values for printed samples (5-12 kPa) are lower than reported moduli (20-55 kPa) for analogous materials described in the literature;[39-41] however, there is variation among reported values due to different sources and grades of both gelatin and TG, as well as different formulations and processing. The low stiffness of the tested samples is attributed to the relatively short cross-linking time and uncertainty in determining

the exact cross sectional area of the gage region. Regardless, the mechanical test results indicate that this material is a soft but resilient hydrogel which responds similarly over multiple extension/retraction cycles; none of the specimens failed during repeated 10 mm stretching cycles. Representative load-displacement curves are included as **Figure** S2 (Supporting Information); variation in the initial toe region is attributed to minor differences in the specimen grip region which absorbs the initial loading with a low apparent stiffness before the gage region begins to deform (the linear region) with an apparent stiffness of 11.9 ± 2.1 kPa based on the dogbone specimens. Visible gaps at filament interfaces are observed to develop during stretching of rectangular printed specimens fabricated with perpendicular print paths; however, complete failure is not observed under these test conditions. Unexpectedly, there is no statistically significant difference between the effective stiffness of printed rectangular specimens with different print path designs (5.5 ± 0.8 kPa for parallel vs. 6.2 ± 1.1 kPa for perpendicular print paths). This indicates that adjacent printed material has time to mix and fuse effectively within the support material before the cross-linking process is complete, which is a distinct advantage of support-material based printing since it enables the fabrication of robust soft structures with mechanical properties essentially independent of the print path design. Other printing methods are more sensitive to the exact print path [38] and may require extensive optimization of print paths to achieve suitable properties in all loaded regions.[42] The reduced effective stiffness of the rectangular specimens compared to dogbone specimens is attributed to stress concentrations arising from this geometry [43] as well as uncertainty in the gage area determination. This is supported by the fact that the effective stiffness of the printed dogbone structure is significantly higher than either of the printed rectangular specimens.

Cell-laden structures are produced by printing cell-laden gelatin/gellan ink in TG-supplemented gellan support materials. As shown in **Figure** 6(a), living fibroblasts are

observed to spread and multiply in gellan-gelatin composite matrices over several days; initially round isolated cells develop elongated morphologies and divide to produce interconnected clusters within the hydrogel construct. A few blue stained nuclei without associated green fluorescence are visible at each time point. Since the blue signal is obscured by intense green fluorescence in live cells, these blue stained nuclei are attributed to dead cells within the matrix. Although preliminary tests show that both gelatin/alginate and gelatin/gellan ink formulations are suitable for fabricating cell-laden structures, cell extension and development of cell-cell contacts is much more rapid in the gellan formulation. This is attributed to the lower overall gelatin concentration as well as to the microscale heterogeneity introduced by gellan microgels. Other work has found that for methacrylated gelatin constructs, cell activity is inversely related to gelatin concentration.[29, 32-34] Cells remain viable, active, and proliferating after printing as indicated by positive staining with fluorescein diacetate, notable cell extension within the first 6 hours and development of extensive cell-cell contacts within the first 24 hours, and appearance of pairs and clusters of cells over time as shown in **Figure** S3(a).

The effect of the printed surface quality on cell behavior is also of interest in the tissue engineering field. Diffuse[10] or irregular[9] surfaces, depending on whether the material remains fluid or is immediately cross-linked upon deposition, have been observed in other types of support bath-enabled printing where both support and ink are aqueous. Because both support and ink are aqueous materials with similar properties, interfacial diffusion and mixing is ubiquitous when cross-linking is delayed; even when cross-linking is immediate, the interface may be irregular since the interfacial tension is too low to induce surface smoothing before gelation takes place.[8] The diffuse surface due to curing in a continuous yield stress support material is unique to this type of fabrication process; other fabrication methods rely on solid molds or immediate cross-linking to define the boundaries of a hydrogel so such interfacial

diffusion is not possible and the hydrogel surface is sharply defined. The effect of this type of diffuse hydrogel surface has not been evaluated in the context of biomedical applications – cell behavior, adhesion, diffusion limits, and tissue integration may all be affected and this is a subject which deserves further attention in a more extensive future study. It is important to understand how the printing process affects cell behavior in order to select appropriate fabrication techniques for a given application.

In this work, a simple morphological examination of fibroblasts seeded on two surfaces (gelatin/alginate cross-linked using TG in air and using TG in gellan as during printing, respectively) as illustrated in **Figure** 6(b) is used to evaluate the effect of this bath-supported fabrication methodology and gellan bath on the cell behavior. Cells seeded on tissue culture polystyrene (TCPS) are also examined as a control as shown in Figure S3(b). Although gelatin/gellan ink is favored for cell-laden structure printing, 10% gelatin with 2% alginate is utilized in this case to avoid the potential effects of the gellan microgels on the surface morphology of the gelled discs. Little difference between the two gelatin surfaces is observed; cell spreading in both cases lags slightly behind TCPS, but in general the cell morphology on the two surfaces is similar at each time point. While the topic merits further investigation for situations where adhesion and tissue integration involving specific cell types and environments are critical for functionality, this evaluation indicates that fibroblasts interact similarly with both types of gelatin surface, whether gelled using TG directly or in the gellan-TG bath.

2.2.2 Structures stabilized by thermal gelation

Printing and thermal gelation of gelatin-based ink structures in the gellan fluid gel support bath is also demonstrated as shown in **Figure** 7 (the lattice cube and branching tube). Herein 5% gelatin + 2% alginate ink was deposited in a 0.5% gellan support bath containing 0.1% $CaCl_2 \cdot 2H_2O$ but without TG. Instead of enzyme-mediated covalent cross-linking, the

ink was solidified by reducing the bath temperature. Gelatin forms a physical hydrogel upon cooling due to aggregation of helical regions, much like gellan. Structures are generally similar to those produced by enzymatic gelation except that they lack thermal stability and liquefy under physiological conditions.

2.2.3 Structures stabilized by ionic cross-linking

To demonstrate the stability of gellan fluid gel support materials in the presence of multivalent ions and resulting suitability for printing ionically cross-linked materials, alginate structures were printed and then stabilized by ionic cross-linking as illustrated in **Figure** 8. A 2% sodium alginate solution in PBS was utilized as the ink material in this set of experiments. Sodium alginate consists of a family of unbranched binary anionic copolymers of 1,4-linked β-D-mannuronic acid (M units) and α-L-guluronic acid (G units). It undergoes gelation when interacting with multivalent ions such as Ca^{2+}. Gelation occurs as such multivalent cations form interchain ionic bonds between G blocks, giving rise to a stable alginate network such as the calcium alginate network shown in the inset of **Figure** 8(a). Alginate structure fabrication is analogous to gelatin structure fabrication: ink is deposited in a 0.5% gellan support formulation containing 0.1% $CaCl_2$•$2H_2O$ but without TG. Instead of incubating printed structures at 37°C for enzymatic cross-linking, the entire support bath is immersed in 2% w/v (136 mM) $CaCl_2$•$2H_2O$ for at least two hours to provide abundant calcium ions for ionic cross-linking. Representative printed structures (spiral cone and branching tube) are shown in **Figure** 8(b). Although cell-laden alginate constructs are feasible using this printing approach, alginate has limited utility for tissue engineering since it is difficult to control degradation and mechanical properties, and it lacks specific sites for cell interaction. Thus, gelatin is selected as a more biologically relevant build material for all cell-laden biomedical constructs.

2.2.4 Structures stabilized by photoinitiated cross-linking

PEGDA-based ink consisting of 10% PEGDA combined with 0.5% gellan fluid gel is also utilized to demonstrate the suitability of 0.5% gellan + 0.1% $CaCl_2 \cdot 2H_2O$ as a support material for structures stabilized by photoinitiated cross-linking as shown in **Figure** 9. Under UV irradiation in the presence of a photoinitiator, the terminal acrylate functional groups on PEGDA polymerize to form cross-links in the form of poly(acrylate) chains that link many PEGDA molecules. While similar print fidelity and quality are obtained for the biopolymer materials (alginate and gelatin) regardless of specific formulation, the PEGDA-based ink is much less robust. The poor printability of the PEGDA+gellan ink is attributed to the low molecular weight of the PEGDA (700 g/mole) as well as its high solubility and mobility in aqueous conditions. Unlike the long polymer chains in the other formulations, which are entangled with one another and relatively slow moving, the short PEGDA chains can diffuse readily into the surrounding support bath since they are too short to become extensively entangled and the rheology modifier (gellan fluid gel) is in the form of microgel particles rather than free polymer chains. Small solid structures such as the spiral cone shown in **Figure** 9 can be printed with reasonable fidelity, but thin walled or filamentous structures such as tubes and lattices are not feasible. Very small, simple textile patterns are also fabricated; this success is attributed to the rapid completion of the fabrication process. The print time for these structures is less than 2 minutes, and they are irradiated within 10 seconds of print completion. Larger structures typically take on the order of 10-20 minutes to complete; by the end of the printing process, the PEGDA in the bottom layers may have diffused into the support material and no recognizable structure can be formed. The gellan support material has little impact on the photoinitiated gel formation of PEGDA structures, except for the diffusion issue noted above. It is likely that the constructs formed using this ink could be improved by UV exposure of each layer as it is printed; however, this would be a fundamentally different printing process since each layer would be cured before the next is

deposited. Therefore, it is not investigated in this work and may be the subject of future research.

2.3 Printing quality analysis

There are a variety of factors which affect the suitability of a support bath material for a particular printing application. Some of the most important aspects for biomedical construct printing are the biocompatibility of the entire process, the structural stability of printed constructs, and the ability to print constructs using extracellular matrix (ECM)-like hydrogels. Process biocompatibility has many facets: it includes a support material which is stable under physiological conditions, a suitable window of printing parameters to minimize cell damage [44, 45] while enabling efficient fabrication, and the ability to separate the printed object from the support material under mild conditions. Structural stability, particularly for hydrogels, is related to both cross-linking and water content. Increased cross-linking leads to increased stability, while increasing water content tends to soften and weaken hydrogels. Thus, cross-linking within the support material is desirable in order to recover intact constructs, but swelling (water uptake) is generally undesirable since it both weakens the structure and distorts the designed geometry; while water loss (de-swelling) is a less severe problem, it does also distort the structure and may impede diffusion of nutrients and waste around embedded cells. Finally, a variety of factors contribute to the printability of hydrogel materials. The precursor must be extrudable in order to form the object; however, the cross-linking process must also be cell compatible and feasible within the support material to stabilize the designed structure before removing it from the support material.

2.3.1 Swelling in gellan bath

Bath supported fabrication is particularly attractive for soft materials including hydrogels which lack the mechanical stiffness to support a free-standing complex structure in air; they may also be prone to desiccation during printing. By printing such materials in an

aqueous support environment, weak materials can be shaped into complex structures without risk of mechanical failure or desiccation during printing. Indeed, it is possible for water to diffuse between the support material and the printed object, resulting in higher or lower water content in the printed object than in the ink used to produce it. While not necessarily damaging to the ink material, such swelling or shrinkage/de-swelling affects the shape fidelity and mechanical properties of the printed object and should be avoided if possible. As shown in Figure S4, printed structures closely match the original design; variations may be attributed to deformation of the soft hydrogel structures under their own weight.

Figure 10 shows the dimensional variation of filaments in various support material formulations (0.5% gellan, 1.0% gellan, 0.5% gellan + 0.1% $CaCl_2$•$2H_2O$, and 4% Laponite EP) normalized to the initial filament width; representative optical micrographs used to quantify this variation are shown in Figure S5. Observations are made over the course of a typical fabrication time of 1 hr to evaluate whether the dimensions of the first layer would change significantly by the time the last layer is printed in a 3D construct. In general, no significant change is observed within one hour; all filaments remain within 10% of their original dimensions. Calcium supplemented support material results in slight shrinkage while calcium-free support materials allow a slight increase in filament width. Lines in Laponite support materials are typically better defined with sharper edges at all time points than those in gellan. This is reasonable since the nanoscale platelets which make up the Laponite support bath tend to have smaller gaps in their packing than the micron-scale particles in the gellan fluid gel support material. Thus, if sharply defined edges are needed, gellan is not ideal. However, soft biomedical structures rarely require such qualities; fuzzy edges are acceptable provided the overall structure is intact. It is speculated that fuzzy surfaces may in fact facilitate tissue integration and interactions with cells on the surface since the surface material is more available for interactions (dangling chains and a sparse network at the surface can

wrap around cells and interact with receptors over a large portion of the cell surface immediately) than on sharply defined flat surfaces (strictly 2D interactions possible). Although a similar evaluation of PEGDA ink filaments is not carried out, it is observed that a delay between printing and UV irradiation resulted in very poor shape fidelity or lack of structure, depending on the design. As aforementioned, this is attributed to rapid diffusion of the relatively small PEG molecules into the surrounding gellan support material, distorting the printed shape and/or diluting the gel precursor to such an extent that gelation is no longer possible.

Because gellan is pre-formed as stable bulk gel material, the amount of water trapped in the rigid gellan network within each microgel is fixed before printing and there is little driving force for water uptake or expulsion. This is distinctly different from support materials like Carbopol, which are prepared by re-hydrating dried microgel particles. In Carbopol, the water content within each particle is limited by the total amount of water present and the flexible polymer network readily absorbs or releases water in response to osmotic pressure gradients. As a result, printed filaments may swell or shrink notably over time depending on the ink and Carbopol support bath compositions. In contrast, dimensional changes in a gellan support bath are attributed to diffusion of the printed polymer between gellan microgels, a much slower process for typical biopolymers. When cross-linking agents are supplied by the support bath, this diffusion is arrested at an early stage since the diffusing polymer chains are the first to encounter the cross-linking agent and form a continuous cross-linked network at the outer edge of the printed material.

2.3.2 Cleaning printed constructs

One aspect of bath-supported printing which is easy to overlook is the removal of support bath materials from a final printed object. Residual support material introduces undesirable variability in the printed objects and reduces the potential for clinical or

commercial use of the technology. Thus, it is important to understand how the support material interacts with the printed material and how to effectively separate them post-fabrication. These characteristics may vary from system to system and critical parameters vary depending on applications; herein the evaluation focuses on the removal of support materials rather than an in-depth analysis of specific and non-specific interactions between support bath and ink. Cleaning printed constructs is in some ways analogous to the post processing step in powder-bed type additive manufacturing, where the raw powder surrounds and fills the printed object as it is fabricated and must be removed once printing is complete. However, while residual powder is often removed by compressed air,[46, 47] blasting,[48] and/or sonication,[49] milder alternatives are required for fragile hydrogel constructs loaded with living cells, which would be damaged structurally by intense washing and biologically by sonication. Prior work has relied on targeted washing [11-13] or dissolution of the support material,[8] but both of these methods have limitations; targeted washing is labor intensive, while support materials which liquefy under physiological conditions limit processing conditions and materials. A support bath which can be removed under milder conditions is needed, especially for fragile biomedical constructs.

In general, gellan fluid gel support material is much easier to remove than Laponite, which is also a versatile support bath material for bioprinting;[13] upon gentle agitation in excess PBS, gellan microgels simply float away leaving macroscopically clean structures as shown in **Movie** M2, while a layer of Laponite remains visible and interior cavities are filled with support material after similar treatment of structures printed in Laponite. This is attributed to the stronger shear thinning behavior of gellan, which results in a transition to a very low viscosity fluid under conditions which do not effectively liquefy the Laponite material. To quantitatively assess support material removal, cylindrical gelatin-based hydrogel tubes (10% gelatin/2% alginate ink) with a diameter of 4 mm and a height of 6 mm are

printed in 0.5% gellan, 1.0% gellan, 4% Laponite EP, or directly into tared vials without support material (as the plain ink control), then thermally gelled, washed, blotted to remove excess water, weighed, and dried to constant mass. Controls do not require washing or blotting since no support material is present initially. 10% gelatin ink is selected to form robust thermal gels and avoid variations related to cross-linking agents supplied by the support bath, such as TG or calcium.

The residual dry mass for each condition is shown in **Figure** 10(b). Both gellan concentrations show slightly increased residual mass compared with the plain ink which may be attributed to salt diffusion from the PBS-based bath into the gel tubes during the gelation and washing procedures and/or to trace amounts of the gellan support materials. However, the residual dry weight of tubes printed in Laponite is much higher, indicating that a significant amount of support material remains adsorbed to the structure's surface after washing. Although effective removal of Laponite from printed structures has been demonstrated,[12, 13] it relies on manual targeted cleaning of features which is labor intensive and may damage fragile features or soft printed materials. For other microgel support materials such as gelatin and Carbopol, removal has not been discussed extensively. Gelatin has been removed by simply raising the temperature to 37°C; however, it is not a suitable support material for printing native gelatin structures since any mechanism to stabilize the printed structure would also cross-link the surrounding support material, making recovery of the printed structure impossible. Carbopol microgels have been removed by exploiting shrinkage at physiological electrolyte concentration; however, it is unclear how efficient this process is since shrinking microgels may simply form a more compact coating on the printed surface rather than washing away. Based on this analysis, rigid fragmented gellan gel particle dispersions serve as optimal support bath materials for printing freeform hydrogel structures with minimal residual support material.

3. Conclusions

This work demonstrates that gellan gum based fluid gel formulations are versatile support bath materials for printing-then-solidification biofabrication. While most of work presented herein is based on the 0.5% gellan fluid gel, the 1.0% gellan fluid gel works very well too for printing applications. Gellan fluid gels enable enzymatic, thermal, ionic, or photoinitiated cross-linking and easy recovery of printed structures while maintaining cell viability and structural fidelity. Although some limitations related to low molecular weight ink materials are identified, the printing process is generally robust and convenient for fabricating hydrogel structures. Furthermore, the reported gellan support material enables facile production of soft, complex, covalently cross-linked, and cell-laden gelatin-based structures suitable for further maturation. Structures are designed and fabricated to demonstrate a range of achievable features in a variety of materials, highlighting the versatility of this support material. Finally, several metrics based on fluid filament stability and construct cleaning have been developed to compare support materials for biofabrication and enable appropriate material selection for optimal results in a given application. Future work includes identifying optimal combinations for printing, the complete characterization of functional gellan gum microgel properties, investigation of the effects of additives on support bath performance, investigation of the resulting printed construct surface quality and its influence on cell behavior, printing and characterization of heterogeneous acellular and cellular structures, and further maturation of cell-laden constructs for tissue engineering applications.

4. Materials and Methods

4.1 Materials

4.1.1 Gellan solution and fluid gel preparation

Three gellan fluid gel formulations were prepared for this study: 0.5% gellan with 0.1% w/v $CaCl_2$•$2H_2O$ was utilized for all printing, while the other two formulations (0.5% gellan without $CaCl_2$ and 1.0% gellan without $CaCl_2$) were prepared for comparison of swelling and rheological behavior. Gellan fluid gels (0.5% and 1.0% w/v gellan) were prepared by dispersing the appropriate mass of low acyl gellan (Kelcogel F low acyl gellan gum, Modernist Pantry, York, ME) in phosphate buffered saline (PBS, Corning cellgro, Manassas, VA) in conical vials, then placing the closed vials in a boiling water bath for at least 20 minutes for full dissolution. After cooling completely, the bulk hydrogel was pressed through a stainless steel mesh (140 mesh, 100 μm holes) for consistent fragmentation. For printing, the 0.5% gellan fluid gel was supplemented with 0.1% w/v $CaCl_2$•$2H_2O$ (6.8 mM, calcium chloride dihydrate, Sigma-Aldrich, St. Louis, MO). Fluid gels were stored at 4°C for up to one week before use. For TG mediated cross-linking of printed gelatin structures, the support material was further supplemented with 2% w/v TG (MooGloo TI, Modernist Pantry, York, ME) and mixed gently immediately before use.

4.1.2 Laponite support material preparation

Laponite support materials (4% EP and 4% w/v XLG) were prepared by dispersing the appropriate mass of Laponite powder (EP or XLG, BYK Additives, Inc., Gonzales, TX) in 40 mL deionized water in a 50 mL conical vial; the mixture was vortexed for 5 minutes and allowed to stand for at least 24 hours before use.

4.1.3 Ink preparation:

In general, inks were prepared by dispersing polymers in PBS as follows.

Gelatin-based ink preparation

Five gelatin-based ink formulations were utilized in this study: 5% w/v gelatin + 2% w/v alginate in PBS (for structure fabrication), 10% gelatin + 2% alginate in PBS (for structure fabrication, mechanical evaluation, and gel surface evaluation), 10% gelatin + 2%

alginate + black pigment (for swelling evaluation), 10% gelatin + 2% alginate in deionized water (for cleaning evaluation), and 4% gelatin + 0.5% gellan + 0.1% $CaCl_2$ (for structure fabrication and biological evaluation). Gelatin + alginate inks were prepared were prepared by dissolving 5% or 10% gelatin (type A, 225 bloom, from porcine skin) along with 2% alginate in PBS at 37°C. 10% gelatin + 2% alginate + black pigment ink was prepared by mixing india ink (Eternal black ink, Higgins, Leeds, MA) 1:4 by volume with deionized water to make a 20 vol% mixture, then dissolving 2% alginate and 10% gelatin in the pigment dispersion at 37°C to make ink with adequate contrast for imaging. Gelatin/gellan ink was prepared by adding the appropriate mass of gelatin to pre-made gellan fluid gel containing 0.1% w/v $CaCl_2 \cdot 2H_2O$ (as described in 4.1.1).

In addition, a 10% w/v solution of gelatin in PBS was prepared for enzyme activity tests by dispersing the appropriate mass of gelatin in PBS and warming to 37°C.

Alginate ink preparation

To prepare 2% w/v alginate ink, the appropriate mass of sodium alginate (alginic acid, sodium salt, Acros Organics, Waltham, MA) was dispersed in PBS and allowed to dissolve fully before printing.

PEGDA ink preparation

Poly(ethylene glycol) diacrylate (PEGDA) ink was prepared by combining PEGDA (M_n 700, Sigma-Aldrich, St. Louis, MO) 1:9 by volume with pre-made 0.5% gellan fluid gel containing 0.1% w/v $CaCl_2 \cdot 2H_2O$ (as described in 4.1.1) and supplementing the mixture with 0.1% w/v lithium acylphosphinate (LAP) (prepared in house based on a published protocol [50]) as a photoinitiator. LAP was selected due to its high efficiency, high penetration depth, and good biocompatibility.

Cellular ink preparation

For cellular structure printing, ink was formulated by resuspending a cell pellet in the gelatin/gellan ink formulation. The ink was prepared as described above in 4.1.3.1 and warmed to 37°C. NIH 3T3 fibroblast cells were harvested and suspended in complete media,[51] then pelleted by centrifuging 5 minutes at 1000 rpm. The supernatant was discarded and replaced with the warm ink mixture to produce ink with final concentrations of 0.5% gellan, 4% gelatin, 0.1% w/v $CaCl_2 \cdot 2H_2O$, and 5 x 10^6 cells/mL in PBS and loaded in a sterile disposable 5 mL syringe for printing. Printing parameters were the same as for cell-free gelatin/gellan ink.

4.2 Rheological characterization of materials

Rheological properties were measured using a rheometer (MCR-702 TwinDrive, Anton-Paar, Graz, Austria) with a 25 mm sandblasted (R_a= 4.75 μm) parallel-plate measuring geometry, 1 mm gap. To determine the yield stress quantitatively, steady rate sweeps were conducted by varying the shear rate from 100 s^{-1} to 0.01 s^{-1}, and the stresses were measured at different shear rates; a pre-shear step at 100 s^{-1} for 30 sec followed by a 1 min rest to recover structure was used to eliminate loading effects. Strain-dependent (0.01-100%), time-dependent (oscillatory shear alternating between 1% and 200% strain at 6.28 rad/sec at 300 sec intervals), and frequency dependent (1% strain, 0.628-628 rad/sec) oscillatory shear data was collected using the same instrument.

4.3 3D printing

For printing, a Hyrel Engine SR (Hyrel3D, Norcross, GA) 3D printer with a CSD-5 (UV array removed for these experiments) or KRA-15 head was utilized with 23 gauge stainless steel tips (Norsdon EFD, Vilters, Switzerland). Custom GCode scripts for simple structures were generated manually; more complex tubular structures were designed using SolidWorks, exported as STL files, and sliced using the embedded Slic3r tools in the Repetrel control software for the Hyrel3D printer. The spiral cone STL file was downloaded from

Thingiverse, healed in MeshLab, and then processed using Slic3r in Repetrel. Typical printing parameters were: layer thickness 0.1-0.15mm, printing speed 2.5-10mm/sec. Optimized material-specific settings for each ink formulation are listed in **Table** S2 (Supporting Information).

Post-printing procedures

For TG cross-linking, the support material was supplemented with TG as described above in 4.1.1; once printing was complete, the support bath with the printed structure was held at 37°C for at least 45 min for gel formation. For thermal gel formation using gelatin inks, the reservoir was stored at 4°C for 2 hours after printing to thoroughly cool the printed structure. For alginate structures, the printing reservoir was immersed in aqueous 138 mM $CaCl_2$ for at least 2 hours before rinsing to recover the ionically cross-linked structure. Finally, PEGDA based structures were immediately irradiated with UV light (Blak-Ray B-100AP, UVP, Cambridge, UK) for 15 minutes.

4.4 Evaluation of support material effects on printing process

To evaluate the dimensional stability of printed material, ink supplemented with black pigment was printed in shallow reservoirs of various support materials and imaged over time; the line width was measured to determine swelling. Brightfield images were captured using the transmitted light channel of a fluorescent microscope (EVOS XL Core, ThermoFisher Scientific, Waltham, MA) and thresholded in ImageJ (NIH, Bethesda, MD); the width of the printed material was measured and data was further processed using Microsoft Excel.

To test cleaning efficiency, hollow tubes were printed in various support materials and dried. The ink for these tests was 10% gelatin + 2% alginate in DI water in all cases, supplemented with blue dye for better visibility. Tubes were printed and the reservoir containing both support material and printed structures was transferred to a refrigerator (4°C) for 30 minutes. Then, the reservoir was immersed in cold PBS and gently agitated to separate

intact gels from the excess support material. Next, the hydrogel structures were blotted dry and weighed, then transferred to tared microcentrifuge tubes (3 structures/ tube) and placed in an 80°C oven and dried to constant mass. For comparison, the same pattern was deposited directly into microcentrifuge tubes (no support material), weighed, and dried. Three cylinders were dried in each microcentrifuge tube for all conditions in order to have sufficient residual mass for accurate mass determination. Constant mass was reached in approximately 3 hr.

Enzymatic activity in various support materials was assessed by casting samples in contact with the various formulations as illustrated in **Figure** 4; this eliminated issues related to cleaning and the printing process. TG was added to pre-prepared support formulations at room temperature with limited mixing to maintain enzymatic activity and used within 2 hr of TG addition. 0.5 mL of each support formulation (gellan, XLG, and EP) was placed in a microcentrifuge tube and centrifuged to achieve a smooth surface. Then, 120 μL of 10% gelatin in PBS was gently pipetted into the tube without disturbing the surface of the support material. The samples were placed in a 37°C bead bath for 60 minutes for enzymatic gelation, if possible, then in a 4°C refrigerator for 45 minutes to thermally gel all samples and enable separation from the support material. Finally, the chilled gels were removed from the vials and rinsed with PBS. They were then soaked in PBS at 37°C to observe whether the gels were thermally stable (covalently cross-linked) or simply physical gelatin gels which dissolve under physiological conditions.

4.5 Mechanical characterization of printed constructs

Tensile mechanical properties of printed samples were measured for comparison. Printed dogbone specimens were designed with nominal gage dimensions of 0.5 mm thick, 6 mm long, and 1.25 mm wide, printed using custom G-code in a gellan support bath supplemented with 2% TG, allowed to cure in the support bath at 37°C, rinsed, and tested without delay. In addition, to evaluate the effects of the print path design, rectangular

specimens (6 mm × 22 mm) with print paths either parallel or perpendicular to the long axis were printed. The 6 mm square grip section at each end had additional layers to facilitate handling, while the central gage region was a single 0.2 mm layer thick and 10 mm long. Specimens were clamped in a micromechanical testing apparatus (eXpert 4000 MicroTester, Admet, Norwood, MA) and stretched at 5 mm/min to a maximum extension of 10 mm. Each sample was subjected to three stretching cycles in rapid succession.

4.6 Biological characterization of printed constructs

Cellular structures were removed from the support material after gelation was complete, rinsed with sterile PBS, and transferred to complete culture media supplemented with antibiotics for incubation in a humidified 37°C incubator. Media was changed every 2 days. For imaging, samples were washed with Dulbecco's phosphate-buffered saline (DPBS, Cellgro, Manassas, VA) twice and stained with a final concentration of 15 μg/mL Hoechst 33342 (Sigma-Aldrich, St. Louis, MO) to stain nuclei blue and a final concentration of 15 μg/mL fluorescein diacetate (FDA) (Sigma-Aldrich, St. Louis, MO) to stain live cells green in 100 μL DPBS. Then, the samples were covered with a cover glass (Fisher Scientific, Pittsburgh, PA) and the images were captured using an EVOS FL inverted fluorescent microscope (Thermo Fisher Scientific, Waltham, MA).

The effect of the printed object surface character on the behavior of seeded cells was assessed by comparing cell morphology on the bottom of a well plate with conventionally cast gelatin surfaces and with gelatin surfaces similar to those produced by printing. For gelatin substrates, a layer of 10% gelatin/2% alginate in PBS was deposited in wells of a 24 well plate; the plate was warmed to ensure full coverage of the surface and allow bubbles to escape. For conventional gelatin surfaces, 20% TG stock was quickly added to a final concentration of 1.0% and carefully mixed with the gelatin layer for consistent gelation and coverage. For simulated printed gelatin surfaces, 0.5% gellan containing 2% TG was gently

added to wells containing the gelatin/alginate mixture, inducing gelation in contact with the support material. The plate was incubated at 37°C for 90 minutes to ensure full gelation, then all gelatin surfaces were rinsed with PBS to remove support material and ensure full hydration. After adding 350 μL complete media, 3T3 cells were deposited on each gel surface as well as in empty wells and their morphology evaluated at 0, 1, 2.5, and 5 hours after seeding.

4.7 Statistical analysis

All quantitative values of measurements in the figures were reported as mean ± one standard deviation (SD) with $n = 3$ samples per group. Statistical analysis was performed using analysis of variance (ANOVA) and p-values of less than 0.05 were considered statistically significant.

Acknowledgements

This research was partially supported by the US National Science Foundation (CMMI-1762941), and access to the Anton Paar rheometer at the University of Florida is appreciated. Cells were cultured by Wenxuan Chai, and the printing process was supported by Chunshan Hu and Yifei Jin.

Supporting Information

Supporting Information is available free of charge from the ACS Applied Materials & Interfaces home page (http://pubs.acs.org/journal/aamick).

Supporting Information: S1: additional rheological characterization of support materials; S2: summary of materials and applications; S3: representative load-displacement curves for mechanical test specimens; S4: cell image comparison; S5: print fidelity evaluation; S6: representative filament images; S7: optimized printing parameters; M1: video of printing in a gellan gum support bath; and M2: video of washing gellan gum from a printed construct.

Author Contributions

A.M.C. and Y.H. conceived the concept of this work, A.M.C. designed and conducted the printing experiments and performed the related analysis, K.S. carried out the rheological testing and characterization, and A.M.C. and Y.H. wrote the manuscript.

Competing Financial Interests

There are no competing financial interests.

References

(1) Huang, Y.; Leu. M.C.; Mazumder, J.; Donmez, A. Additive Manufacturing: Current State, Future Potential, Gaps and Needs, and Recommendations. *ASME J. of Manufacturing Sci. Eng.* **2015**, *137*, 014001-1-10.

(2) Zhang, Z.; Jin, Y.; Yin, J.; Xu, C.; Xiong, R.; Christensen, K.; Ringeisen, B.R.; Chrisey, D.B.; Huang, Y. Evaluation of Bioink Printability for Bioprinting Applications. *Appl. Phys. Rev.* **2018**, *5*, 041304.

(3) Murphy, S.V.; Atala, A. 3D Bioprinting of Tissues and Organs. *Nat. Biotech.* **2014**, *32,* 773-785.

(4) Lee, J.M.; Yeong, W.Y. Design and Printing Strategies in 3D Bioprinting of Cell-Hydrogels: A Review. *Adv. Healthcare Mater.* **2016**, *5*, 2856–2865.

(5) Lee, V.K.; Dai, G. Printing of Three-Dimensional Tissue Analogs for Regenerative Medicine. *Ann. Biomed. Eng.* **2017**, *45*, 115-131.

(6) Huang, Y.; Schmid, S.R. Additive Manufacturing for Health: State of the Art, Gaps and Needs, and Recommendations. *ASME J. of Manufacturing Sci. Eng.* **2018**, *140*, 094001.

(7) Bhattacharjee, T.; Zehnder, S.M.; Rowe, K.G.; Jain, S.; Nixon, R.M.; Sawyer, W.G.; Angelini, T.E. Writing in the Granular Gel Medium. *Sci. Adv.* **2015**, *1*, e1500655.

(8) Hinton, T.J.; Jallerat, Q.; Palchesko, R.N.; Park, J.H.; Grodzicki, M.S.; Shue, H.J.; Ramadan, M.H.; Hudson, A.R.; Feinberg, A.W. Three-Dimensional Printing of Complex Biological Structures by Freeform Reversible Embedding of Suspended Hydrogels. *Sci. Adv.* **2015**, *1*, e1500758.

(9) Hinton, T.J.; Hudson, A.; Pusch, K.; Lee, A.; Feinberg, A.W. 3D Printing PDMS Elastomer in a Hydrophilic Support Bath via Freeform Reversible Embedding. *ACS Biomater. Sci. Eng.* **2016**, *2*, 1781-1786.

(10) Jin, Y.; Compaan, A.; Bhattacharjee, T.; Huang, Y. Granular Gel Support-Enabled Extrusion of Three-Dimensional Alginate and Cellular Structures. *Biofabrication* **2016**, *8*, 025016.

(11) Hajash, K.; Sparrman, B.; Guberan, C.; Laucks, J.; Tibbits, S. Large-Scale Rapid Liquid Printing. *3D Printing and Additive Manufacturing* **2017**, *4*, 123-132.

(12) Jin, Y.; Chai, W.; Huang, Y. Printability Study of Hydrogel Solution Extrusion in Nanoclay Yield-Stress Bath During Printing-Then-Gelation Biofabrication. *Mat. Sci. Eng. C*. **2017**, *80*, 313-325.

(13) Jin, Y.; Compaan, A.M.; Chai, W.; Huang, Y. Functional Nanoclay Suspension for Printing-then-Solidification of Liquid Materials. *ACS Appl. Mater Interfaces*. **2017**, *9*, 20057-20066.

(14) Moxon, S.R.; Cooke, M.E.; Cox, S.C.; Snow, M.; Jeys, L.; Jones, S.W.; Smith, A.M.; Grover, L.M. Suspended Manufacture of Biological Structures. *Advanced Materials* **2017**, *29,* 1605594.

(15) O'Bryan, C.S.; Bhattacharjee, T.; Hart, S.; Kabb, C.P.; Schulze, K.D.; Chilakala, I.; Sumerlin, B.S.; Sawyer, W.G.; Angelini, T.E. Self-Assembled Micro-Organogels for 3D Printing Silicone Structures. *Sci. Adv.* **2017**, *3*, e1602800.

(16) Prajapati, V.D.; Jani, G.K.; Zala, B.S.; Khutliwala, T.A. 2013. An Insight into the Emerging Exopolysaccharide Gellan Gum as a Novel Polymer. *Carbohydr*. *Polym*. **2013**, *93*, 670-678.

(17) Osmałek, T.; Froelich, A.; Tasarek, S. Application of Gellan Gum in Pharmacy and Medicine. *Int. J. Pharm. (Amsterdam, Neth.)*. **2014**, *466*, 328-340.

(18) Stevens, L.R.; Gilmore, K.J.; Wallace, G.G. Tissue Engineering with Gellan Gum. *Biomat. Sci.* **2016**, *4*, 1276-1290.

(19) García, M.C.; Alfaro, M.C.; Muñoz, J. Creep-Recovery-Creep Tests to Determine the Yield Stress of Fluid Gels Containing Gellan Gum and Na+. *Biochem. Eng. J.* **2016**, *114*, 257-261.

(20) García, M.C.; Alfaro, M.C.; Muñoz, J. Rheology of Sheared Gels Based on Low Acyl-Gellan Gum. *Food Sci. Technol. Int.* **2016**, *22,* 325-332.

(21) Adams, S.; Frith, W.J.; Stokes, J.R. Influence of Particle Modulus on the Rheological Properties of Agar Microgel Suspensions. *J. Rheol.* **2004**, *48*, 1195-1213.

(22) Morris, E.R.; Nishinari, K.; Rinaudo, M. Gelation of Gellan–a Review. *Food Hydrocolloids* **2012**, *28*, 373-411.

(23) Pérez-Campos, S.J.; Chavarría-Hernández, N.; Tecante, A.; Ramírez-Gilly, M.; Rodríguez-Hernández, A.I. Gelation and Microstructure of Dilute Gellan Solutions with Calcium Ions. *Food hydrocolloids* **2012**, *28*, 291-300.

(24) Kirchmajer, D.M.; Steinhoff, B.; Warren, H.; Clark, R. Enhanced Gelation Properties of Purified Gellan Gum. *Carbohydr. Res.* **2014**, *388*, 125-129.

(25) Gutowski, I.A. The Effects of pH and Concentration on the Rheology of Carbopol Gels. Ph.D thesis, Simon Fraser University, Burnaby, British Columbia, 2010.

(26) Di Giuseppe, E.; Corbi, F.; Funiciello, F.; Massmeyer, A.; Santimano, T.N.; Rosenau, M.; Davaille, A. Characterization of Carbopol® Hydrogel Rheology for Experimental Tectonics and Geodynamics. *Tectonophysics* **2015**, *642*, 29-45.

(27) Eshtiaghi, N.; Yap, S.D.; Markis, F.; Baudez, J.C.; Slatter, P. Clear Model Fluids to Emulate the Rheological Properties of Thickened Digested Sludge. *Water Res*. **2012**, *46*, 3014-3022.

(28) Chen, P.Y.; Yang, K.C.; Wu, C.C.; Yu, J.H.; Lin, F.H.; Sun, J.S. Fabrication of Large Perfusable Macroporous Cell-Laden Hydrogel Scaffolds Using Microbial Transglutaminase. *Acta Biomater.* **2014**, *10*, 912-920.

(29) Irvine, S.A.; Agrawal, A.; Lee, B.H.; Chua, H.Y.; Low, K.Y.; Lau, B.C.; Machluf, M.; Venkatraman, S. Printing Cell-Laden Gelatin Constructs by Free-Form Fabrication and Enzymatic Protein Cross-Linking. *Biomed. Microdevices* **2015**, *17*, 16.

(30) Kolesky, D.B.; Homan, K.A.; Skylar-Scott, M.A.; Lewis, J.A. Three-Dimensional Bioprinting of Thick Vascularized Tissues. *Proc. Nat. Acad. Sci. U.S.A.* **2016**, *113*, 3179-3184.

(31) Yang, G.; Xiao, Z.; Long, H.; Ma, K.; Zhang, J.; Ren, X.; Zhang, J. Assessment of the Characteristics and Biocompatibility of Gelatin Sponge Scaffolds Prepared by Various Crosslinking Methods. *Sci. Rep.* **2018**, *8*, 1616.

(32) Nichol, J.W.; Koshy, S.T.; Bae, H.; Hwang, C.M.; Yamanlar, S.; Khademhosseini, A. Cell-laden Microengineered Gelatin Methacrylate Hydrogels. *Biomaterials* **2010**, *31*, 5536-5544.

(33) Yue, K.; Trujillo-de Santiago, G.; Alvarez, M.M.; Tamayol, A.; Annabi, N.; Khademhosseini, A. Synthesis, Properties, and Biomedical Applications of Gelatin Methacryloyl (GelMA) Hydrogels. *Biomaterials* **2015**, *73*, 254-271.

(34) Klotz, B.J.; Gawlitta, D.; Rosenberg, A.J.; Malda, J.; Melchels, F.P. Gelatin-Methacryloyl Hydrogels: Towards Biofabrication-Based Tissue Repair. *Trends Biotech.* **2016**, *34*, 394-407.

(35) Xavier, J.R.; Thakur, T.; Desai, P.; Jaiswal, M.K.; Sears, N.; Cosgriff-Hernandez, E.; Kaunas, R.; Gaharwar, A.K. Bioactive Nanoengineered Hydrogels for Bone Tissue Engineering: a Growth-Factor-Free Approach. *ACS Nano* **2015**, *9*, 3109-3118.

(36) Matricardi, P.; Cencetti, C.; Ria, R.; Alhaique, F.; Coviello, T. Preparation and Characterization of Novel Gellan Gum Hydrogels Suitable for Modified Drug Release. *Molecules* **2009**, *14*, 3376-3391.

(37) Reed, K.; Li, A.; Wilson, B.; Assamoi, T. Enhancement of Ocular In Situ Gelling Properties of Low Acyl Gellan Gum by Use of Ion Exchange. *J. Ocul. Pharmacol. Ther.* **2016**, *32*, 574-582.

(38) Christensen, K.; Compaan, A.; Chai, W.; Xia, G.; Huang, Y. In Situ Printing-then-Mixing for Biological Structure Fabrication Using Intersecting Jets. *ACS Biomater. Sci. Eng.* **2017**, *3*, 3687-3694.

(39) Kim, Y.J.; Uyama, H. Biocompatible Hydrogel Formation of Gelatin From Cold Water Fish Via Enzymatic Networking. *Polym. J.* **2007**, *39*, 1040-1046.

(40) McCain, M.L.; Agarwal, A.; Nesmith, H.W.; Nesmith, A.P.; Parker, K.K. Micromolded Gelatin Hydrogels for Extended Culture of Engineered Cardiac Tissues. *Biomaterials* **2014**, *35*, 5462-5471.

(41) Bettadapur, A.; Suh, G.C.; Geisse, N.A.; Wang, E.R.; Hua, C.; Huber, H.A.; Viscio, A.A.; Kim, J.Y.; Strickland, J.B.; McCain, M.L. Prolonged Culture of Aligned Skeletal Myotubes on Micromolded Gelatin Hydrogels. *Sci. Rep.* **2016**, *6*, 28855.

(42) Yerazunis, W.S.; Barnwell III, J.C.; Nikovski, D.N. Strengthening ABS, Nylon, and Polyester 3D Printed Parts by Stress Tensor Aligned Deposition Paths and Five-Axis Printing. *Proceedings of the Solid Freeform Fabrication Symposium, Austin, Texas.* 2016, *10.*

(43) Feng, L.; Jasiuk, I. Effect of Specimen Geometry on Tensile Strength of Cortical Bone. *J. Biomed. Mater. Res., Part. A*. **2010**, *95*, 580-587.

(44) Yin, J.; and Huang, Y. Study of Process-Induced Cell Membrane Stability in Cell Direct Writing. *ASME J. of Manufacturing Sci. Eng.* **2011**, *133,* 054501-1-5.

(45) Zhang, Z.; Chai, W.; Xiong, R.; Zhou, L.; Huang, Y. Printing-induced Cell Injury Evaluation during Laser Printing of 3T3 Mouse Fibroblasts. *Biofabrication* **2017***,* 9, 025038-1-12.

(46) Partee, B.; Hollister, S.J.; Das, S. Selective Laser Sintering Process Optimization for Layered Manufacturing of CAPA® 6501 Polycaprolactone Bone Tissue Engineering Scaffolds. *J. of Manufacturing Sci. Eng.* **2006**, *128*, 531-540.

(47) Williams, C.B.; Cochran, J.K.; Rosen, D.W. Additive Manufacturing of Metallic Cellular Materials Via Three-Dimensional Printing. *The International Journal of Advanced Manufacturing Technology* **2011**, *53*, 231-239.

(48) Eldesouky, I.; Harrysson, O.; West, H.; Elhofy, H. Electron Beam Melted Scaffolds for Orthopedic Applications. *Additive Manuf*. **2017**, *17*, 169-175.

(49) Wysocki, B.; Idaszek, J.; Szlązak, K.; Strzelczyk, K.; Brynk, T.; Kurzydłowski, K.J.; Święszkowski, W. Post Processing and Biological Evaluation of the Titanium Scaffolds for Bone Tissue Engineering. *Materials* **2016**, *9*, 197.

(50) Fairbanks, B.D.; Schwartz, M.P.; Bowman, C.N.; Anseth, K.S. Photoinitiated Polymerization of PEG-Diacrylate with Lithium Phenyl-2, 4, 6-trimethylbenzoylphosphinate: Polymerization Rate and Cytocompatibility. *Biomaterials* **2009**, *30*, 6702-6707.

(51) Xu, C.; Chai, W.; Huang, Y.; Markwald, R. R. Scaffold-Free Inkjet Printing of Three-Dimensional Zigzag Cellular Tubes. *Biotechnol. Bioeng*. **2012**, *109*, 3152−3160.

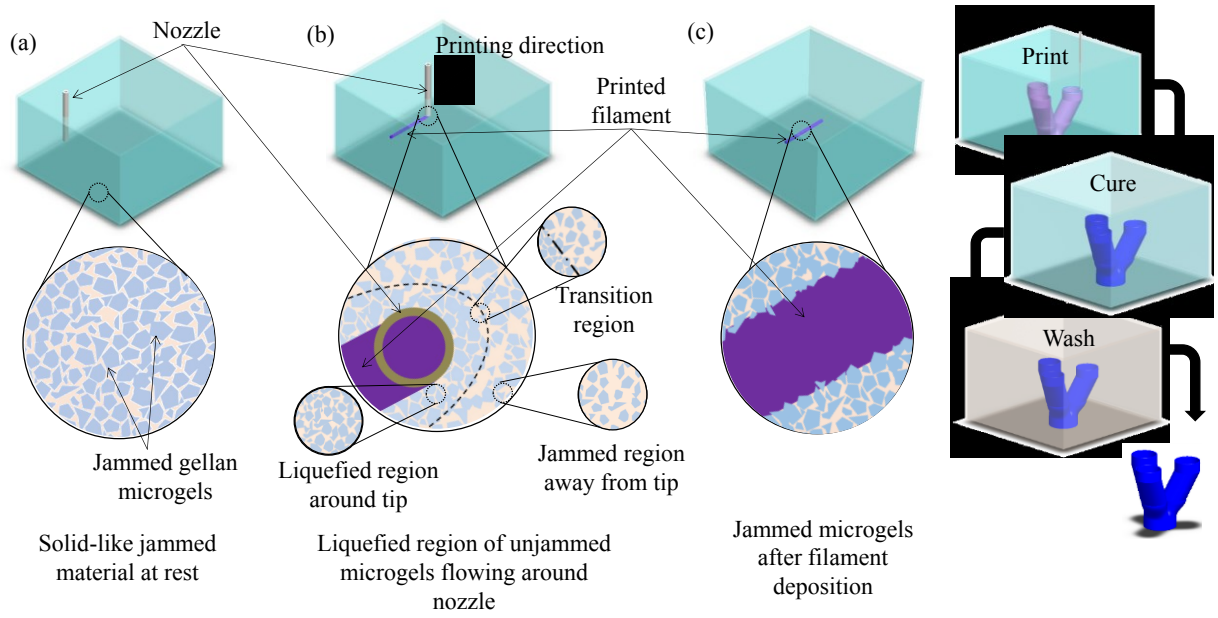

Figure 1. Printing process schematics of print bath (a) before printing, (b) during filament deposition showing local liquefaction, and (c) after filament deposition showing entrapped filament as well as (d) overall printing and post-processing steps to fabricate a branching tubular construct.

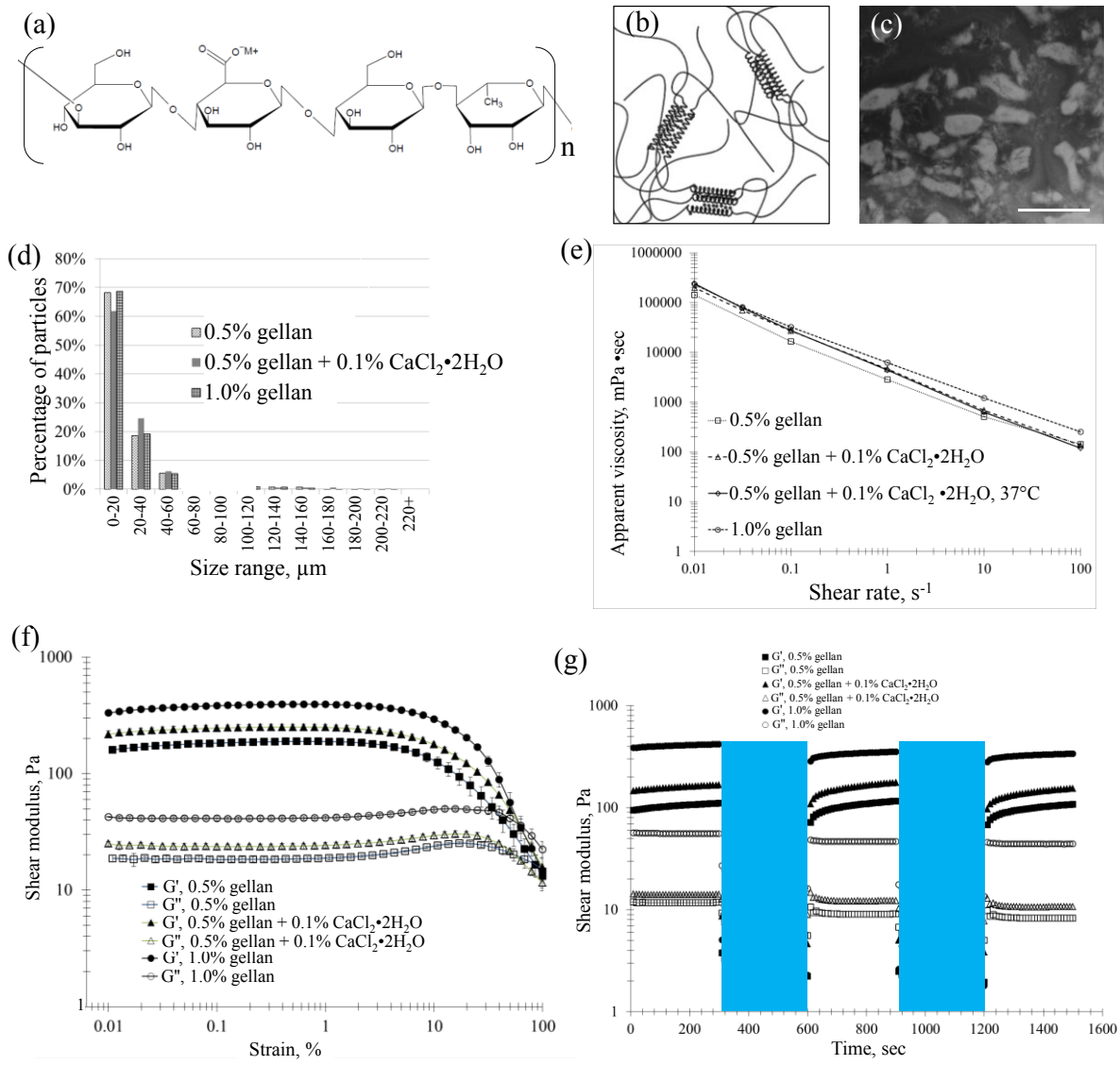

Figure 2. Microstructure and rheology of gellan fluid gel (a) gellan chemical structure, (b) schematic of gel formation by aggregation of helical sections of gellan molecules, (c) typical gellan gum microgels in excess water for observation of individual particles and aggregates, (d) size distribution for gel particles in each support formulation, (e) steady shear rheology, (f) oscillatory strain-dependent rheology, and (g) cyclic transition between solid-like and fluid-like behavior (oscillatory shear alternating between 1% and 200% (shaded) strain at 6.28 rad/sec).

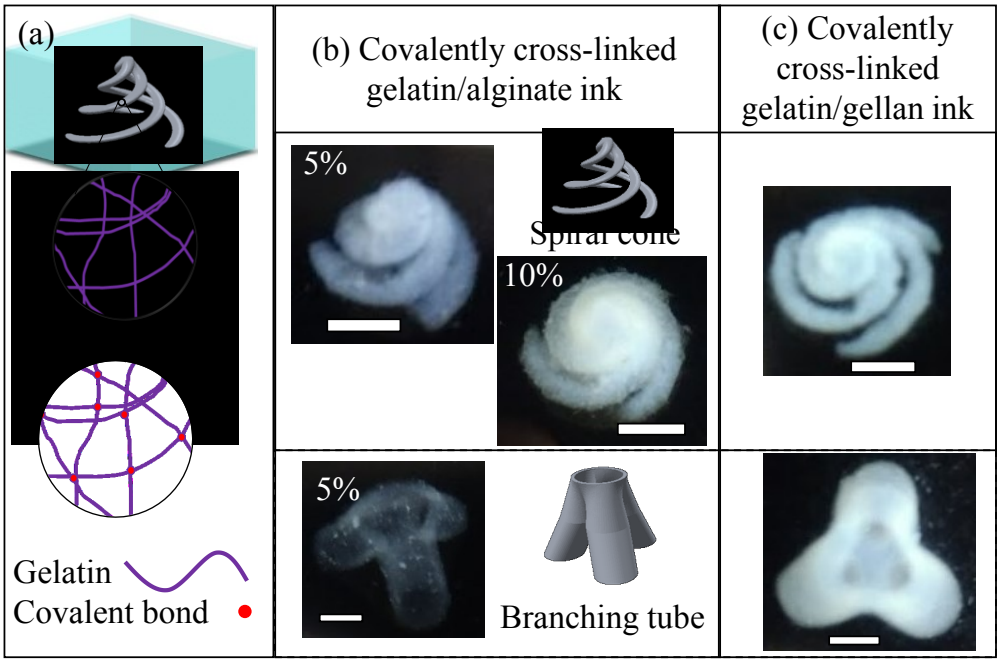

Figure 3. Enzyme-mediated covalent cross-linking results (a) schematic of printing and cross-linking mechanism, (b) gelatin+alginate structures stabilized by enzyme mediated covalent cross-linking, and (c) gelatin+gellan structures stabilized by enzyme-mediated covalent cross-linking (scale bars: 5 mm).

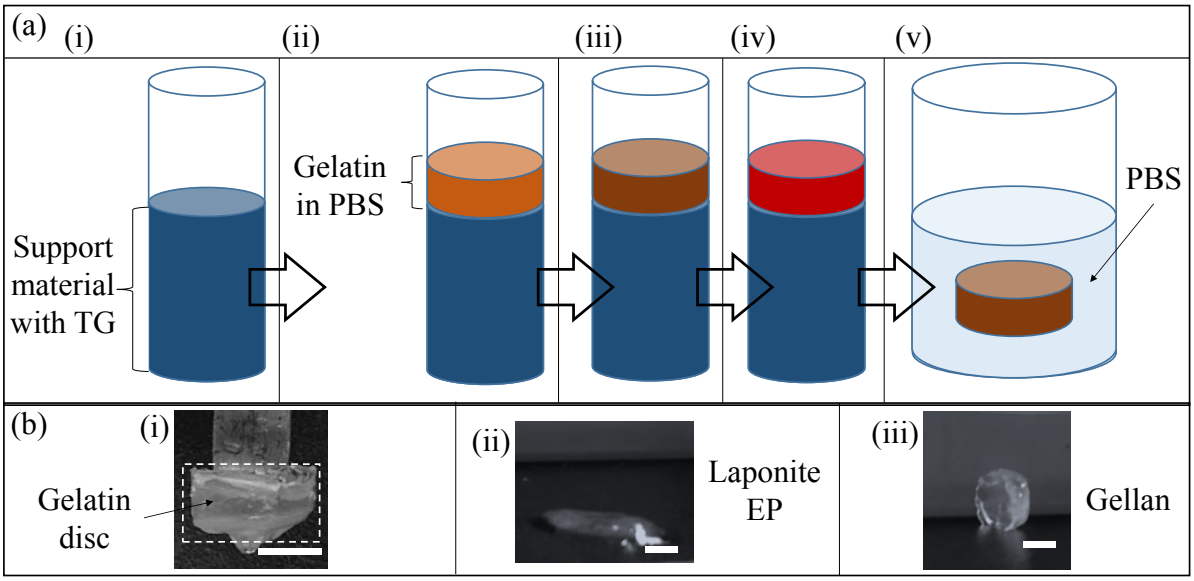

Figure 4. Evaluation of gelation: (a) support material enzyme activity evaluation process (i) prepare support material in vial and centrifuge to generate smooth surface, (ii) gently add a layer of gelatin solution to the vial, (iii) incubate 60 min at 37°C for TG cross-linking, if TG is active, (iv) transfer to refrigerator (4°C) for 45 min to form physical gel, and (v) transfer gel to 37°C PBS (without support material) and observe stability/dissolution; (b) images of gels cross-linked (i) thermally in air, (ii) by TG from Laponite EP, and (iii) by TG from gellan (scale bars: 5mm).

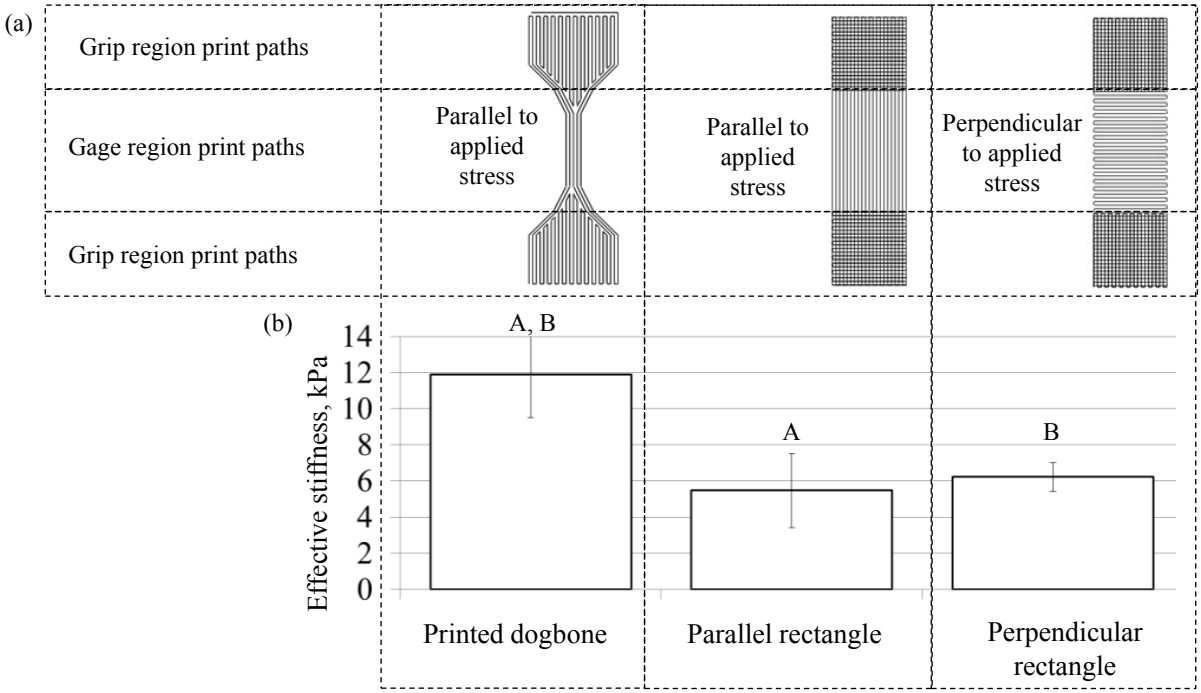

Figure 5. Mechanical property evaluation: (a) print paths for test specimens and (b) measured effective stiffness for printed specimens (there is a statistically significant difference between conditions marked with the same letter).

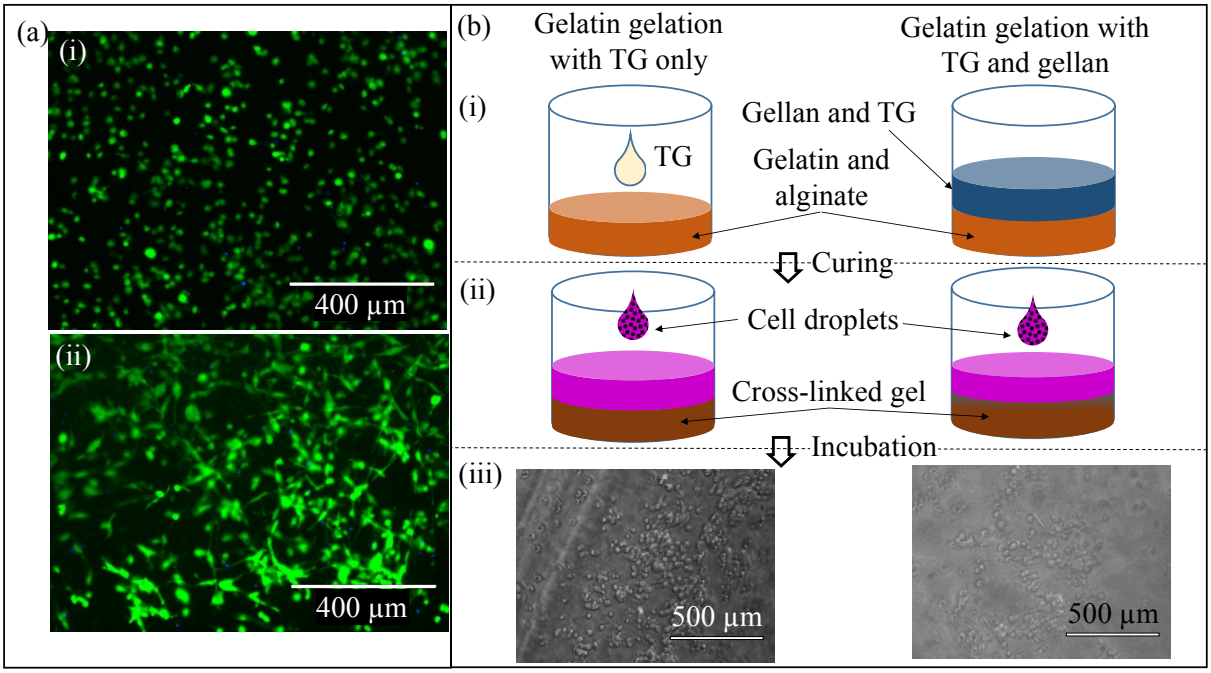

Figure 6. 2D and 3D cell culture: (a) fibroblast morphology and viability in 3D constructs (i) 24 and (ii) 72 hr after gelation (all cell nuclei are stained blue; in living cells, the blue fluorescence is obscured by the intense green signal from the live cell stain, so isolated blue fluorescence indicates dead cells) and (b) production of different gel surface types (conventional and simulated printed surfaces) and resulting cell morphologies after incubation (i) Prepare gels with conventional or diffuse surfaces, (ii) rinse surfaces and seed cells, and (iii) observe morphology after incubation for 5 hr.

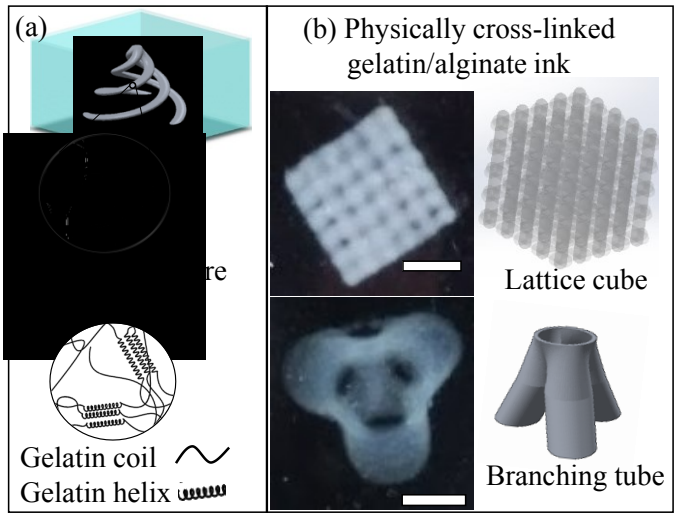

Figure 7. Temperature-dependent physical cross-linking results: (a) schematic of printing and cross-linking mechanism, and (b) gelatin + alginate structures stabilized by physical gelation (scale bars: 5 mm).

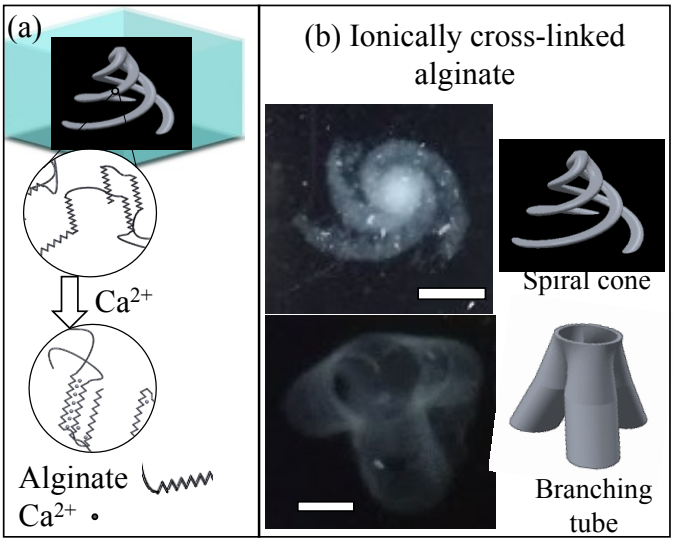

Figure 8. Calcium-mediated ionic cross-linking results: (a) schematic of printing and cross-linking mechanism, and (b) alginate structures stabilized by ionic cross-linking (scale bars: 5 mm).

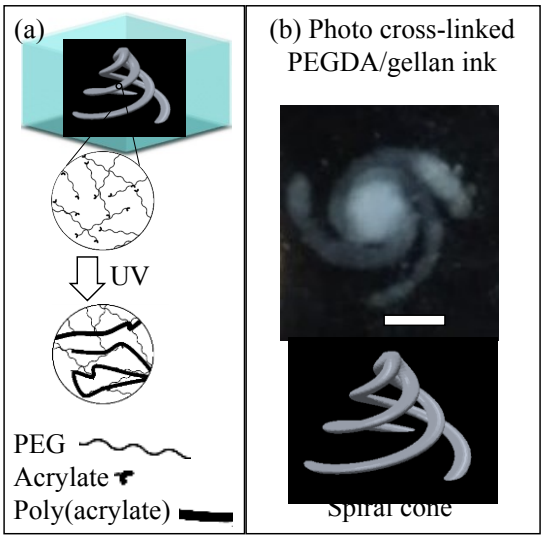

Figure 9. UV-initiated covalent cross-linking results: (a) schematic of printing and cross-linking mechanism and (b) PEGDA + gellan structure stabilized by photoinitiated covalent cross-linking (scale bar: 5 mm).

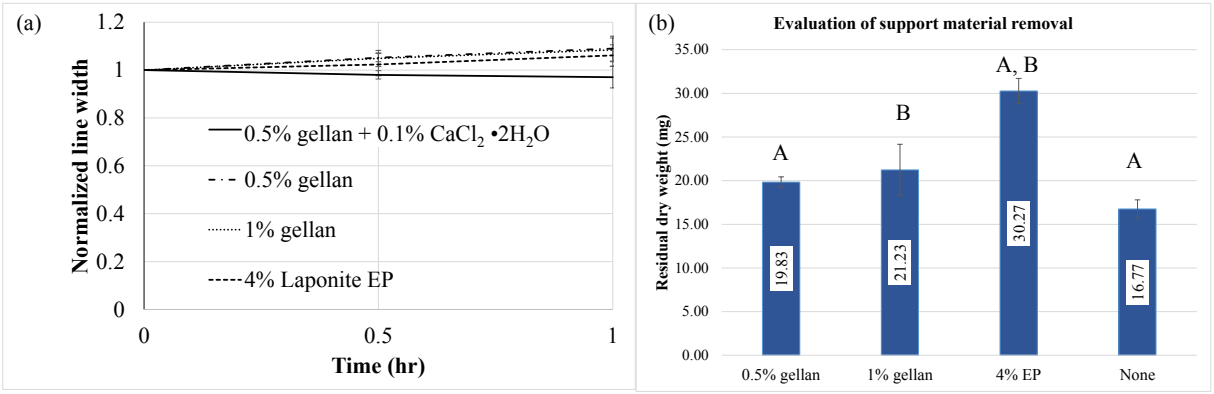

Figure 10. Printing process evaluation: (a) filament dimensional stability and (b) evaluation of support material removal (there is a statistically significant difference between conditions marked with the same letter).

Table 1. Herschel-Bulkley fitting parameters for various gellan fluid gel support formulations

Material	σ_0 (Pa)	K	n
0.5% gellan + 0.1% $CaCl_2 \cdot 2H_2O$, 37°C	1.9	2.04	0.35
0.5% gellan + 0.1% $CaCl_2 \cdot 2H_2O$	1.1	3.15	0.29
1.0% gellan	1.5	4.38	0.35
0.5% gellan	1.3	1.25	0.51

TOC